The respiratory health hazard of tephra from the 2010 Centennial eruption of Merapi with implications for occupational mining of deposits

The respiratory health hazard of tephra from the 2010 Centennial eruption of Merapi with implications for occupational mining of deposits

Damby, D.E.[1], Horwell, C.J.[1], Baxter, P.J.[2], Delmelle, P.[3], Donaldson, K.[4], Dunster, C.[5], Fubini, B.[6], Murphy, F.A.[4], Nattrass, C.[1], Sweeney, S.[7], Tetley, T.D.[7], Tomatis, M.[6]

[1] Institute of Hazard, Risk and Resilience, Department of Earth Sciences, Durham University, Science Labs, South Road, Durham, DH1 3LE, UK.

[2] Institute of Public Health, University of Cambridge, Cambridge, CB2 2SR, UK.

[3] Earth & Life Institute, SST/ELI/ELIE - Environmental Sciences, Université catholique de Louvain, Croix du Sud 2 bte L7.05.10, B-1348 Louvain-la-Neuve, Belgium.

[4] The University of Edinburgh/MRC Centre for Inflammation Research, The Queen's Medical Research Institute, Edinburgh, EH16 4TJ, UK.

[5] MRC-HPA Centre for Environment and Health, King's College London, 150 Stamford Street, London, SE1 9NH, UK.

[6] Dipartimento di Chimica I.F.M., Interdepartmental Center “G. Scansetti” for Studies on Asbestos and other Toxic Particulates, Università degli studi di Torino, Via P. Giuria 7, 10125, Torino, Italy.

[7] Lung Cell Biology, National Heart and Lung Institute, Imperial College London, Dovehouse Street, London SW3 6LY, UK.

Abstract

Ashfall into heavily populated areas during the October-November 2010 eruption of Merapi volcano, Indonesia created anxiety regarding the growing impacts to health as the eruption escalated and the hazard zone widened. We made a preliminary assessment of the respiratory hazards to human health of the tephra deposits (ashfall, lahar, and PDC surge) from the eruption using a laboratory protocol specifically developed to study the toxic potential of volcanic ash particles. Twenty samples collected from a range of locations were analysed for health-pertinent mineralogical parameters (grain size, crystalline silica content, morphology, surface area, bulk chemistry, and leachable elements) and bio-reactivity (hydroxyl radical generation, haemolytic potential, oxidative capacity, pro-inflammatory response). The grain size pertinent to respiratory health was variable, ranging from 1.4–15.6 vol. % sub-4 μm and 3.0–28.9 vol. % sub-10 μm diameter material. No fibre-like particles were observed. Cristobalite was present in all samples, ranging from 1.9-9.5 wt. %, but surface reactivity and *in vitro* toxicity assays showed low reactivity for all samples tested. The risk of direct exposure to ash from fallout was in any case low due to seasonal rains limiting its re-suspension and the immediate and effective clean-up of communities by local people who supplied the ash to the Indonesian construction industry for use as aggregate. However, mining of the lahar and thick PDC deposits in the valleys draining the volcano is performed on a vast, industrial scale which could result in high occupational exposure to thousands of sand miners at Merapi during the dry seasons. Further study of the health hazard of the mined Merapi deposits is warranted.

Abbreviations

PDC – Pyroclastic density current

BAF – Block-and-ash flow

NGO – Non-governmental organisation

IVHHN – International Volcanic Health Hazards Network

CVGHM - Centre for Volcanology and Geological Hazards Mitigation

1. Introduction

Merapi volcano, located in Central Java, Indonesia, is one of the most persistently active volcanoes in the world, and has a history of deadly eruptions in the last century occurring every 3-5 years. Today, there are 1.1 million people living on its slopes. Merapi has displayed both explosive and effusive activity throughout its eruptive history; however, activity over the last 225 years has been dominated by the viscous extrusion of basaltic-andesite lava domes and subsequent small gravitational, or explosive, dome collapse (Camus et al., 2000), producing pyroclastic density currents (PDCs) with associated plumes. Lava dome eruptions have been interspersed with explosive events every 26-58 years (Camus et al., 2000; Thouret et al., 2000). The most common, potentially lethal hazards are lahars, which result in damage far beyond the more immediate area affected by dome collapse (Thouret et al., 2000).

The October-November 2010 explosive eruption of Merapi was its largest since 1872, when there were reports of up to 30 cm of ashfall, and caused its worst disaster since 1930, when 36 villages were destroyed and 1369 people killed in PDCs. Major explosions on 26 October, 30-31 October, and 4-5 November dispersed large amounts of ash to the west and south, affecting major urban areas of Magelang and Yogyakarta. The total erupted tephra volume was estimated to be 50-100 x 10^6 m^3, approximately 10 times greater than deposits from typical eruptions of the past few decades (Lavigne et al., 2011; Surono et al., this volume). Varying contributions of juvenile dome and older 2006 dome material were incorporated into the discrete eruptive events (Surono et al., this volume). PDCs and associated detached surges extended beyond the previously delineated hazard zones (Thouret et al., 2000), resulting in the destruction of some villages and 367 official fatalities (Gertisser, 2011; Surono et al., this volume). Nearly a third of a million people were displaced due to the risk of PDC impact to their villages, and many of these individuals would be exposed to re-suspended ash throughout the clean-up and rebuilding phase.

Quarrying of the extensive lahar and PDC deposits for construction began soon after the 2010 eruption and continued on an industrial scale involving thousands of people from local villages and further afield. In response to the immediate and future hazard posed by the erupted material, we embarked on a laboratory assessment of the respiratory health hazard of Merapi ash found in

different tephra deposits (ash fall, a detached surge, and a lahar) following a protocol previously developed at Rabaul, Papua New Guinea, Chaitén, Chile and Eyjafjallajökull, Iceland (Horwell et al., In Prep-b; Horwell et al., 2010a; Le Blond et al., 2010) (see Figure 1). Health-pertinent mineralogical data of grain size, bulk composition, particle morphology, and crystalline silica content are combined with toxicological assays (surface hydroxyl radical generation, particle oxidative capacity, haemolysis, pro-inflammatory response) to inform the particle hazard.

1.1 Potential diseases related to the inhalation of volcanic ash

Horwell & Baxter (2006) give a comprehensive review of respiratory diseases associated with inhaling volcanic ash particles <10 µm diameter. Following immediate exposure, susceptible individuals may develop asthma and bronchitis (Baxter et al., 1983); heavy and prolonged exposure to ash containing a high concentration of crystalline silica in the 'respirable' fraction (<4 µm diameter and able to penetrate to the lung alveoli) may lead to the fibrotic lung disease silicosis and possibly lung cancer (International Agency for Research on Cancer, 1997). In addition, pulmonary tuberculosis is common in Indonesia and its incidence and severity can be promoted by heavy exposure to dusts containing crystalline silica (Hnizdo and Murray, 1998). It is well understood that substantial quantities of crystalline silica can crystallise in volcanic domes as cristobalite through vapour-phase deposition and devitrification of groundmass, e.g. up to 20 wt. % in ash from both the Soufrière Hillls volcano on Montserrat, West Indies (Baxter et al., 1999; Horwell et al., In Prep-a) and Chaitén, Chile (Horwell et al., 2010a). Eruptions at dome forming volcanoes can generate extremely fine-grained ash (Horwell, 2007), and can further contain cristobalite through incorporation of altered edifice material in an explosive event (Baxter et al., 1999; Horwell et al., 2010a).

1.2 Evidence of crystalline silica generation at Merapi

Cristobalite has previously been identified in volcanic ash near Merapi, with a particular emphasis on its presence in volcanic soils (Hardjosoesastro, 1956). However, no studies have quantified the concentration of cristobalite or addressed it as a respiratory hazard. Archived samples were therefore informative at the onset of the 2010 eruption. Analysis of an ash sample from a 1998 dome collapse event (named MER_arc in this study, see Table 1) raised concerns about the amount of respirable material produced by Merapi, with this sample containing 13 vol. % sub-4 µm particles (Horwell, 2007)

but only 3.8 wt. % cristobalite (Table1). Before this study, we also analysed the cristobalite content of dome rock samples from 1996 and 1998 block-and-ash flows (BAFs) and confirmed the presence of cristobalite (3-5 wt. %). Cristobalite content in dome rock is expected to be substantially lower than that in co-PDC plume deposits due to enrichment of cristobalite in the plume by fractionation (Horwell et al., 2001).

1.3 Initial response to the eruption

When international news agencies began reporting health-related problems attributed to exposure to volcanic ash (27 October) it became clear that rapid dissemination of information on preparedness for ashfall and the health hazards of ash was warranted. The International Volcanic Health Hazard Network (www.ivhhn.org) is a recognized source of such advice, and IVHHN fact sheets were rapidly translated for us into Bahasa Indonesia by a native speaker. High-resolution copies were sent for local printing by NGOs, such as Save the Children, for widespread distribution at the evacuation camps. We sought ash samples for analysis from these contacts and others at Universitas Gadjah Mada, Jogjakarta, with the first batch of samples arriving at Durham University on 18 November 2010, weeks before Indonesia's Centre for Volcanology and Geological Hazards Mitigation (CVGHM) reduced the activity warning from its highest level, level 4. Local scientists and NGOs collected fresh ash fall samples at 10 discrete locations, but it was not possible to co-ordinate a systematic sampling strategy in the emergency period. We undertook a field mission to collect further samples and to monitor air quality in populated areas.

2. Materials and methods

2.1 Sample collection and selection

Samples from three different types of tephra deposits were collected, namely ash fall, a detached surge and a lahar, to provide insight into the hazard posed by variably-sourced ash at Merapi. Eleven ash fall samples were collected by local scientists and volunteers between 30 October and 13 November 2010. A further 9 samples were collected during our field mission from 29 November to 11 December 2010 from *in situ* village and field deposits. The village investigated (Bronggang) had been impacted by two detached PDC surges and samples were taken both outside and within affected houses. Although efforts were made to collect samples as fresh as possible, many samples were rained on prior to collection. The eruption took place during the wet season and normal rainfall may have been augmented by the 2010 La Niña event. During this time heavy rain fell on the region for more than 2 hours per day. A complete listing of samples is presented in Table 1, and sample locations are displayed in Figure 2. Nine samples collected after the 5 November eruption are likely composite samples from the different major eruptive events as the plume pattern for the 5 November eruption overlaid portions of the deposits from both the 25 October and 30 October eruptions. Samples MER_10_01, MER_10_03 and MER_10_04 were collected prior to being rained upon. Samples MER_10_13 through _15 are detached surge samples, where MER_10_13 and _14 were collected from elevated surfaces (1 m) and correspond with floor-collected samples MER_10_12 and _15, respectively.

Mineralogical analyses were performed on samples in accordance with the described protocol (Figure 1). A set of four samples (MER_10_02, MER_10_03, MER_10_04, and MER_10_12) was selected as a representative cross section for additional surface reactivity and toxicology analyses based on eruption date, exposure to the environment following deposition, and potential hazard defined by grain size and crystalline silica data. Imaging was performed on the four sub-samples as well as MER_10_01, a freshly collected ash sample, and MER_10_13, the fine surge component associated with MER_10_12. An archived sample (MER_arc), collected pristine 200m from a PDC on the slopes of Merapi during a dome collapse eruption in 1998 (Horwell, 2007; Horwell et al., 2007), was included for comparison.

All samples were oven dried in glass dishes at 90 °C for 24 hours and then sieved through 2 and 1 mm mesh sieves to remove any material that is too coarse for laser diffraction grain size analysis. Unless otherwise stated, all samples used for analysis are the sub-1 mm fraction in order to keep results directly comparable to previous studies.

2.2 Mineralogical and compositional analyses

All of the methods in the health-hazard assessment protocol have been previously described (Le Blond et al., 2010) with the exception of inflammatory potential and are only discussed briefly here.

Grain-size distribution of volcanic ash is important as particles with <10 μm aerodynamic diameter are able to penetrate into the human lung (Quality of Urban Air Review Group, 1996). Measurements were carried out using a Malvern Mastersizer 2000 laser diffractometer with a Hydro MU attachment at the Department of Geography, University of Cambridge, UK after Horwell (2007). This technique measures particles within the 0.2-2000 μm range and data reported are the average of three measurement cycles (Table 2). Samples were measured with a refractive index of 1.63 and an absorption coefficient of 0.1 (Horwell, 2007). Results were rescaled to incorporate the 1-2 mm fraction of the ash using the fraction weights measured after sieving. All samples contained <<1.0 wt. % 1-2 mm fraction except for samples MER_10_07 (7.21 wt. %), MER_10_11 (4.09 wt. %), MER_10_16 (11.27 wt. %) and MER_10_20 (5.57 wt. %). Only samples MER_10_11 and MER_10_16 contained substantial >2 mm material at 6.17 wt. % and 7.33 wt. %, respectively; however, this material is outside of the ash fraction and is not further discussed in this study.

The major elemental oxide composition of samples MER_10_01 through _12 was determined using X-ray fluorescence (PANalytical Axois Advanced X-ray fluorescence (XRF) spectrometer at the Department of Geology, University of Leicester, UK).

Scanning electron microscopy (SEM) was used to investigate particle morphology. Particles mounted on polycarbonate discs adhered to Al stubs and coated with 30 nm of gold/palladium were imaged using the Hitachi SU-70 FEG SEM at the Department of Physics, Durham University, UK.

The total quantity of crystalline silica as quartz, cristobalite, and tridymite was determined by X-ray diffraction (XRD) at the Natural History Museum, London following the Internal Attenuation Standard (IAS) method of Le Blond et al. (2009) using an Enraf-Nonius X-ray diffractometer with an INEL curved position sensitive detector (PSD). This method allows for the rapid quantification of a single mineral phase (e.g., a crystalline silica polymorph) in a mixed dust without prior knowledge of the mineralogical composition of the bulk sample. The method has a < 3 wt. % error.

Leachate analyses were carried out on a sample split that was not oven-dried as it is possible that drying can alter surface volatile species. The concentrations of readily-soluble elements in the ash were determined by gently shaking 0.25 g of ash with 25 ml of deionized water for 1 hour. The pH of the ash leachate was measured prior to filtration on 0.2 µm membrane filter. Anions (F^-, Cl^-, SO_4^-) and major elements (Si, Al, Fe, Mg, Ca, Na, K) were measured in the filtrated ash leachate by ion chromatography (IC) and inductively-coupled plasma-optical emission spectroscopy (ICP-OES), respectively. Trace metals (As, Cd, Co, Cr, Cu, Ni, Pb and Zn) were determined by inductively coupled plasma-mass spectroscopy (ICP-MS).

2.3 Surface reactivity and *in vitro* toxicity testing

The specific surface area (SSA) of a particle is an indicator of the total available surface for reactions to occur in the lung. Surface area for the selected subset of 4 samples was measured using the Brunauer-Emmett-Teller (BET) method of nitrogen adsorption on a Micromeritics TriStar 3000 Surface Area and Porosimetry Analyser in the Department of Chemistry, Durham University, UK. Prior to analysis samples were degassed under N_2 at 150° C for at least 2 hours.

Particle surface reactivity can be estimated by the ability of a particle to generate reactive oxygen species (Fubini et al., 1995). Horwell et al. (2007; 2003a) suggest that all volcanic ash is capable of generating the hydroxyl radical via the iron-catalysed Fenton reaction, with more mafic samples being able to elicit a more pronounced response. Electron Paramagnetic Resonance (EPR) spectroscopy in association with the 'spin trap' technique was used to quantify the generation of hydroxyl radicals by the samples in solution through replication of Fenton chemistry (Fubini et al., 1995; Horwell et al.,

2007; Horwell et al., 2003a). Measurements were carried out on a Miniscope 100 ESR spectrometer, Magnettech, at the Dipartimento di Chimica, Università degli Studi di Torino, Italy following a standard methodology (Horwell et al., 2007). Measurements are collected at 10, 30, and 60 minutes, and data are averages of three individual experiments expressed per unit surface area.

The amount of removable ferrous (Fe^{2+}) and ferric (Fe^{3+}) iron on the sample surfaces was determined as this represents the iron available for participation in the Fenton reaction. Removable iron was measured spectrophotometrically at 562 nm using the chelator Ferrozine to remove ferrous iron from the particle surface (Horwell et al., 2007; Horwell et al., 2003a). Total iron mobilised was measured by first reducing Fe^{3+} to Fe^{2+} with ascorbic acid. Samples were analysed in a Uvikon spectrophotometer also at the Dipartimento di Chimica, Università degli Studi di Torino. Experiments were carried out for 9 days with measurements taken every 24 hours (excluding the weekend). In addition to the four Merapi samples chosen, four ash samples from other volcanoes, analysed previously by Horwell et al. (2007), were re-analysed here for comparative purposes. Data are presented alongside results from Horwell et al. (2007) for Min-U-Sil quartz standard and MER_arc.

The capacity of ash to cause cell membrane damage was determined by lysis of human erythrocytes (red blood cells) sourced from fresh venous blood. Ash samples were diluted in saline to final concentrations between 0.031 and 1.0 mg ml^{-1} and sonicated for 10 minutes. Particle suspensions were incubated with isolated erythrocytes for 30 minutes at room temperature, shaking gently. Following incubation, plates were centrifuged at 400 x *g* for 5 minutes and the amount of released haemoglobin was determined by absorbance at λ=550 nm. The quartz standard DQ12 was used as a positive control and rutile TiO_2 as a negative control. Percentage haemolysis compared to complete haemolysis (0.1 % Triton X-100) was calculated and results are the average of three experiments, each performed in triplicate.

The potential of ash to induce oxidative stress by the depletion of antioxidants in artificial preparations of human respiratory tract lining fluid (RTLF), a measure of bio-reactivity in the airways thought to be associated with asthma (Ayres et al., 2008), was determined at Kings College London. The RTLF exposure assay comprises a composite solution containing a final concentration of 200 μM ascorbic

246 acid (AA), urate (UA) and reduced glutathione (GSH), which was exposed to 50 µg ml^{-1} ash or
247 particulate matter controls (in-house negative (M120) and positive (NIST1648a and roadside PM1-3))
248 for 4 hours at 37 ^{o}C. The post-exposure concentrations of AA, UA and GSH were indicators of the
249 oxidative potential of the ash samples.
250
251 The pro-inflammatory potential of ash was assessed against human lung epithelial type 1-like (TT1)
252 cells (van den Bogaard et al., 2009) to establish their acute and chronic cellular reactivity. Analyses
253 were performed at the National Heart and Lung Institute, Imperial College London. TT1 cells were
254 grown to confluence in DCCM-1 cell culture media with 10 % New Born Calf serum (Invitrogen,
255 Paisley, UK), 1% penicillin/streptomycin/glutamine (Invitrogen) and 0.5 mg ml^{-1} gentacin (G148;
256 Sigma Aldrich). Cells were serum starved for 24 hours prior to sample treatment, and cell monolayers
257 were exposed to tephra samples dispersed in serum-free DCCM-1. Mediator conditioned cell culture
258 medium including the sample doses was removed after 24 hours and centrifuged. Exposed TT1 cell
259 cultures were washed x3 with PBS and fresh cell culture medium was added. Conditioned media
260 removal was repeated at 24 and 72 hours post exposure. Acute (24 hour exposure) and chronic (24
261 and 72 hours post exposure) inflammatory potential was determined by measuring the release of
262 interleukin 6 (IL-6), interleukin 8 (IL-8) and monocyte chemotactic protein (MCP-1) from exposed TT1
263 cells using an enzyme-linked immunosorbent assay (ELISA). A dose range of 0.5 to 50.0 µg ml^{-1} of
264 tephra sample was used.
265
266 **2.4 Ambient air particle concentrations and personal exposure**
267 Ambient air particle concentrations were collected during the field mission using a TSI DustTrak
268 Aerosol Monitor. The instrument was run for 30 minutes each morning and evening in Yogyakarta for
269 9 days as well as at a selection of field sites for short-term (20 minute) ambient readings.
270 Measurements in Yogyakarta were taken at 3 locations: by a main street with heavy traffic, near a
271 school away from major traffic but with frequent foot traffic, and in a quiet neighbourhood with little
272 traffic (1 car every five minutes). Concentrations were also measured in urban air at Magelang,
273 Muntilan, and Klaten. Rural locations monitored were near Selo, Dukun, Argo Mulyo, and Prambanan
274 temple.
275

We monitored the personal exposure for 2 workers while they were extracting river bed deposits and wearing a TSI Sidepak Personal Aerosol Monitor. Two TSI DustTraks were set up concurrently with the personal measurements; one near the working area to collect proximal occupational levels resulting from re-suspension of the deposit, and the other at a distance upwind to collect environmental background levels. All instruments were calibrated prior to use to ensure that directly comparative readings were obtained. We were unable to monitor exposure for the main mining activities on the PDCs because large-scale excavation of material had not yet begun during the field mission.

3. Results

3.1 Particle size

Grain size data are presented as a cumulative volume percent according to health pertinent size fractions (Horwell, 2007) (Table 2). Overall, grain size distributions for the 14 ashfall samples varied in the amount of respirable ash (<4 μm diameter) from 1.4–15.6 vol. %. Aside from a sample from the 26 October eruption which had 15.6 vol. % sub-4 μm material, the rest of the samples' ranges are typical for respirable material generated during Vulcanian to Plinian (VEI 3-4) explosive eruptions (<~10 vol. % sub-4 μm) (Horwell, 2007; Horwell et al., 2010a; Horwell et al., 2010b; Le Blond et al., 2010). Inferring differences in grain size between the major explosive events of the 2010 eruption is difficult, however, due to the effects of sample location distance from the crater, plume dispersal axis and reworking of material by rain.

Detached surge deposits collected from within 2 homes in Bronggang village were, in general, much finer grained than the ash fall and parent surge deposits, with approximately 13 vol. % sub-4 μm material. The component of the detached surges which comprised the samples collected from elevated surfaces within the homes was especially enriched in fines, with 19 vol. % sub-4 μm material (2 samples). This differed greatly from the sample collected from the exterior of the house which only contained 6.5 vol. % sub-4 μm material, although sheltered and appeared pristine when collected, suggesting the coarsest material settles in the parent surge outside of the houses (Jean-Christophe Komorowski, personal communication).

The sample from the lahar deposit was collected 22 km from the crater and contained no ash particles <10 μm. The lahar sample was not investigated further as there was no respirable component.

3.2 Particle morphology

The general morphology of the health-pertinent fractions (sub-10 μm) of Merapi ash was poorly vesiculated, sub-angular and blocky with varying amounts of sub-micron particles adhering to the surfaces of larger particles (Figure 3), as found in samples from other volcanoes (Hillman et al., 2012; Horwell and Baxter, 2006; Horwell et al., 2010a; Horwell et al., 2010b; Le Blond et al., 2010). No

morphological differences were observed between the PDC samples and the fall samples. No respirable mineral fibres were observed in any of the samples, eliminating the asbestiform concern raised from health studies of other eruptions (discussed further in Le Blond et al. (2009) and Reich et al. (2009)).

3.3 Bulk composition

Ash samples ranged from trachy-basalt to trachy-andesite (51.90-57.42 wt. % SiO_2, 1.97-2.42 wt. % K_2O) and are reported on a total alkali versus silica plot (Figure 4). Bulk oxide elemental data for all samples are listed in Table 3. The majority of erupted products at Merapi are calc-alkaline, high-K basaltic-andesites that range from 52-57 wt. % SiO_2 and 1.80-2.84 wt. % K_2O (Camus et al., 2000; Gertisser and Keller, 2003); the array observed in this study encompasses the full range previously reported, and corresponds with bulk rock data of juvenile blocks from the 5 November pyroclastic flows (Surono et al., this volume). While the bulk composition from the 26 and 30 October eruptions reflects the narrowly constrained whole rock data from the 2006-2008 eruptive period (~55-56 wt. % SiO_2 versus ~55-57 wt. % SiO_2 for the current data), ash samples collected from the 5 November eruption appear to be more primitive, with 52-55 wt. % SiO_2. However, there is no evidence of chemical or petrologic changes throughout the eruption in bulk rock samples collected by other scientists (John Pallister, personal communication). Further, deconvolving the effects of environmental exposure from the eruptive phase is difficult as all but one sample from 5 November were composite samples or had been rained on. The apparent discrepancy could be the result of winnowing from wind and rain, especially since the major element composition of the dry 5 November sample (i.e., MER_10_03) overlaps with the 5 November PDC results of Surono et al (this volume). A rough correlation was seen between grain size (sub-4 μm) and bulk SiO_2 (R^2=0.80, data not shown) for wet/composite samples, where finer samples correspond with higher bulk SiO_2 values. This could indicate removal of a fine groundmass fraction from the deposits, which is typically high in silica (e.g., ~70 wt. % SiO_2 for groundmass glass for Merapi 2010). The removal of a fine, vesicular glassy component is consistent with the observation that fall-deposits are dominantly composed of angular, lithic fragments (John Pallister, personal communication). The lower SiO_2 observed could also be the result of physical fractionation in the plume (Horwell et al., 2001), however no correlation was observed between bulk SiO_2 and collection distance.

3.4 Crystalline silica content

Cristobalite was detected in all samples (1.9-9.5 wt. %) and minor amounts of quartz were quantifiable in samples MER_10_06 (1.25 wt. %), _16 (0.75 wt %), and _18 (0.66 wt. %). No tridymite was identified in any sample. Abundances of cristobalite reported in Table 2 are for sieved bulk samples (<1 mm) rather than the respirable fractions as it is not feasible to separate sufficient respirable material with such small quantities of ash (often <20 g) and within the timeframe of an urgent study. The finer, PDC surge samples collected from raised surfaces in houses (MER_10_13 and _14) were depleted in crystalline silica compared to their ground-collected counterparts (MER_10_12 and _15) (3.2 and 4.5 wt. % versus 7.9 and 8.8 wt. % respectively).

3.5 Leachate analysis

The Merapi ash leachates for the subset of 4 samples displayed slightly acidic pH values (5.1-6.3) (table 4). There is no observable difference in pH between wet and dry samples. Calcium was the dominant dissolved cation in all samples. Sulphate was present in higher concentration than Cl^- and F^-. The molal S/Cl ratio in MER_10_02 and MER_10_12 leachates is approximately four times higher than in MER_10_03 and MER_10_04. Copper and Zn were the most abundant trace metals mobilized upon exposure to water. Nickel and Cr were also measured in significant concentrations (0.2 – 1 mg kg^{-1}) in the leachates, while concentrations of Fe, Cd, and Pb were about ten times lower. Compared to other samples, Zn was ten times greater in MER_10_03. This sample is also enriched in Cr and Ni. There were no discernible differences between wet and dry samples, however only one wet sample was analysed (MER_10_02).

3.6 Particle specific surface area

The specific surface area for the selected ash samples ranged from 0.51–1.03 $m^2 g^{-1}$ (Table 2), which is at the low end of the range previously observed for explosive volcanic ash (0.2-6.9 $m^2 g^{-1}$) (Horwell et al., 2007; Horwell et al., 2010b). The PDC surge samples MER_10_12 and MER_10_02 had the greatest surface area per mass and also contained the greatest proportion of respirable material.

3.7 Hydroxyl radical generation and iron release

374 Surface reactivity determined by hydroxyl radical generation for samples MER_10_02, _03, _04 and
375 _12 was low with reference to comparative ash samples analysed concurrently (Figure 5). All four
376 samples generated fewer than 0.1 µmol m^{-2} at 30 minutes with little change in kinetics through each
377 individual experiment. The data follow the expected trend observed in previous studies, where mafic
378 samples generate more hydroxyl radicals than more silicic samples (Horwell et al., 2007; Horwell et
379 al., 2003a). Considering results from tephra fall samples only, the most mafic sample (MER_10_03)
380 generated the greatest number of radicals, whereas the most silicic sample (MER_10_02) generated
381 the fewest radicals. The low overall Fe-catalysed surface reactivity for all samples is unlikely
382 explained by exposure to rain (e.g. Fubini et al. (1995), Fubini (1998), Le Blond et al. (2010)) as
383 MER_10_03 was collected fresh and generated a similar number of radicals to samples exposed for 5
384 days (0.094 µmol m^{-2}). The 1998 dome collapse ash sample MER_arc analysed by Horwell et al
385 (2007) gave similar results to the present study. All samples produced more radicals than the Min-U-
386 Sil quartz standard, and data are consistent with all previously analysed volcanic ash samples
387 (Hillman et al., 2012; Horwell et al., 2007; Horwell et al., 2003a; Horwell et al., 2010b).
388
389 The amount of total iron released for the 4 Merapi samples was on the order of that released by the
390 sample comparisons from Montserrat (andesitic) and Pinatubo (dacitic), and far lower than that
391 released by the Etna and Cerro Negro samples (both basaltic) (Figure 5). No trend was observed for
392 preferential mobilisation of either Fe^{2+} or Fe^{3+} for any of the samples, with MER_10_02 releasing
393 more Fe^{2+}, MER_10_03 releasing more Fe^{3+}, and MER_10_04 and _12 releasing equivalent
394 quantities of both (data not shown for brevity).
395
396 A comparison of hydroxyl radical generation and total iron released (Figure 5) shows very little
397 correlation. As has been seen with other data, there seems to be a lack of trend between iron in either
398 oxidation state (data not shown) or total iron and hydroxyl radical generation when iron release is low
399 (Hillman et al., 2012; Horwell et al., 2007). Production of hydroxyl radicals via Fenton chemistry is a
400 catalytic reaction related to the coordination of iron atoms, and, as such, even trace amounts of Fe^{2+}
401 may be sufficient to trigger hydroxyl radical generation.
402
403 **3.8 *In vitro* toxicology**

None of the samples showed haemolytic activity at the doses used when compared to a positive quartz control. This is in accord with previous reports for the haemolytic potential of other explosive ash samples (Horwell et al., In Prep-b; Le Blond et al., 2010). No significant difference was observed between tephra fall samples and the PDC surge sample analysed.

The ash samples did not exhibit an oxidative potential within the RTLF exposure model. The in-house negative and positive controls performed as expected. Again, this is in line with work carried out on volcanic ash from other volcanoes (Horwell et al., In Prep-b; Le Blond et al., 2010).

Merapi ash was found to be largely non-reactive against the TT1 cell model, failing to incite an acute inflammatory response or impart a lasting (chronic) inflammatory effect following exposure. Three tephra fall samples used in the experiment (MER_10_02, _03, and _04) did not produce a significant increase in cytokine or chemokine release over the unexposed controls. The PDC surge deposit sample (MER_10_12) did produce a significant 1.4-fold increase in MCP-1 at the 24 hour acute exposure, and a significant 1.2-fold increase in IL-8 at 24 hours post acute exposure, however this response was only associated with the highest dose (50 μg ml^{-1}) and resolved by Day 5.

3.9 Ambient air monitoring

Particle concentrations measured in the ambient air at Magelang and Yogyakarta were low and less than anticipated from the resuspension of ash by traffic due to the rapid removal and transport of ash by locals to sell as aggregate, in addition to seasonal rains washing the ash away. In Magelang (26 km WNW), where up to 5 cm of ash was reported during the eruption, nearly all of the ash had been removed or incorporated into the environment prior to the field mission.

No background information on daily concentrations of particulate matter <10 μm (PM_{10}) levels was available for comparison with the data collected during our field mission. The measurements we took may not be representative of all districts surrounding Merapi, but we had no volcano-specific respiratory health concerns as ambient PM_{10} concentrations outside of urban areas were at or below 0.05 mg m^{-3}. Twice daily measurements of ambient concentrations in Yogyakarta and three discrete measurements in Magelang did not rise above 0.10 mg m^{-3} (0.07–0.10 mg m^{-3} in the morning and

0.04-0.05 mg m^{-3} in the afternoon) except for a couple of weekdays (7-9 Dec) in Yogyakarta when construction work was taking place nearby (approximately 1 km away), and concentrations reached upwards of 0.80 mg m^{-3}. Air quality limits are further discussed in section 4.1.

Personal exposure levels for two workers manually shovelling wet ash that had been dredged out of a river using hand tools were 0.055 mg m^{-3} and 0.029 mg m^{-3} (PM_{10}, 1 hour average). Maximum concentrations as one minute averages within those readings were 0.224 mg m^{-3} and 0.175 mg m^{-3}, respectively. Ambient concentrations in the working area were 0.042 mg m^{-3} for a continuous 2 hour reading (PM_{10}), and background monitoring levels at a distance of 100 m (no wind) were 0.022 mg m^{-3}. These results were not representative of exposure conditions for the mining of lahar or PDC deposits in the dry season, but were typical for working with wet ash.

4. Discussion

4.1 Tephra fall and corresponding particle hazard

Work by Surono et al. (this volume) suggests that the 26 October eruption had a phreatomagmatic component. The directed explosion also destroyed part of the existing dome from 2006 (as evidenced by the non-juvenile lithic material present in the associated PDC deposit; Surono et al., this volume). The combination of a phreatomagmatic explosion and disruption of an existing dome likely resulted in the unusually fine grain size distribution of samples from 26 October despite the eruption being regarded as less energetic than the 5 November event. Incorporation of dome material has been shown to produce finer ash than plinian or vulcanian explosive magmatic eruptions where no dome is present, with dome collapse eruptions expected to generate ash with 10-18 vol. % sub-4 µm (Horwell, 2007; Horwell et al., 2010a). Correspondingly, the finest grained samples are from the first eruption on 26 October as well as later composite samples which include ash from the 26 October eruption, i.e. samples MER_10_17 and _18. Sample MER_10_02 from 26 October is exceptionally fine grained (28.9 vol. % sub-10 µm, 15.6 % sub-4 µm); compared to our data base of results for ash from other volcanoes, it is the finest of 250 samples after two samples from the final phreatomagmatic stages of plinian and sub-plinian eruptions at Mt Vesuvius (Horwell, 2007; Horwell et al., 2010b) and a dome-collapse sample form Chaitén volcano in 2008 (Horwell et al., 2010a).

The 5 November eruption also destroyed a dome which had been growing between 31 October and 4 November, yet evidence of this is not distinguishable in the grain size or cristobalite data while accounting for distance of sample collection. This absence of observable indicators of dome incorporation could have been due to integration of tephra from other eruptive events or by the effects of the seasonal climate as most samples associated with that eruption had been exposed to the environment prior to collection.

Previous analysis of a 1998 archive sample before the eruption alerted us to the potential respiratory hazard of the exceptionally fine-grained ash in Merapi's dome eruptions. However, the rapidity with which cities and the surrounding environment recovered from the extensive amount of tephra fall was unforeseen and indeed unprecedented in our experience. This was largely due to the rapid and

475 effective removal of deposited material by local people to sell as aggregate for construction and the
476 daily downpours of rain, which mobilised massive amounts of material from roads and around houses
477 and limited re-suspension shortly after each eruptive event. There was therefore little risk of long-term
478 exposure to the ash for the general population.
479
480 Health guidelines on airborne particulate levels for volcanic ash were developed for Montserrat based
481 on the UK standard for ambient PM_{10} (Expert Panel on Air Quality Standards, 1995; Expert Panel on
482 Air Quality Standards, 2001) and the US occupational exposure limit for crystalline silica (National
483 Institute of Occupational Health and Safety (NIOSH), 2002). Searl et al. (2002) adjusted for 24 hour
484 exposure in the general population of Montserrat as a guide to limiting exposure, recommending no
485 action at concentrations below 0.05 mg m^{-3} and raised alertness for individuals who have experienced
486 adverse health effects during past dusty episodes for concentrations between 0.05-0.10 mg m^{-3} (1
487 hour averages for PM_{10}). The guidelines developed for Montserrat were based on a cristobalite
488 concentration of up to 20 wt. % in the ash and are therefore not directly applicable; however, rural
489 PM_{10} concentrations near Merapi were never measured above 0.05 mg m^{-3} (30 minute readings) at
490 the locations studied, reducing concerns of elevated volcanically-associated PM. Urban PM_{10}
491 concentrations were between 0.04-0.10 mg m^{-3} (30 minute readings, excluding days when
492 construction was taking place in the area), however these above background levels were most likely
493 due to vehicle emissions.
494
495 **4.2 PDC surges and hazard to displaced populations**
496 The only detached surge deposits investigated were from the 5 November eruption in Bronggang
497 village. The substantial grain size differences between the surge deposits collected outside of houses
498 compared with samples collected indoors, however, emphasizes the nature of the hazard. Ash
499 entered houses through ventilation gaps in the walls and below the roofs, preferentially excluding the
500 coarser, basal layer of the surge. One-quarter (23.3 and 25.5 vol. %) of the sample volume for 2
501 samples collected from indoor floor deposits were in the sub-10 µm fraction. Additionally, more than
502 one-third (35.3 and 35.7 vol. %) of the 2 samples collected from 1 metre surfaces inside homes where
503 some people died was sub-10 µm. Only 2 people were inside a house at the time the surge struck
504 and survived their thermal injuries; both were diagnosed as having possible inhalation burns to the

505 respiratory tract. Twenty-five bodies were retrieved by rescuers from inside houses and eighteen from
506 outside; 11 others died in, or on the way, to hospital, but their location at the time of injury was not
507 known. Inhalation of fine ash in hot surges (>300 °C) into the small airway combined with severe
508 burns to the body has a bad prognosis (Kobayashi et al., 1993).
509
510 Fresh surge-related deposits in protected indoor environments are substantially finer than the outdoor
511 surge deposit and airfall tephra measured at Merapi or any other volcanoes (Horwell, 2007). Results
512 from previous studies on ash particles from Montserrat comparing grain-size and crystalline silica in
513 BAFs and corresponding co-PDC plume deposits (Horwell et al., 2001; Horwell et al., 2003b) suggest
514 that the finer surge deposits from raised surfaces, which stayed lofted for longer, would be enriched in
515 cristobalite compared to their corresponding bulk floor samples; however, the opposite was observed
516 in the Merapi samples. As many of the affected houses remained standing, if damaged and ash
517 covered, these indoor deposits are a post-eruption source of exposure during the clean up and
518 rebuilding process. Floors, walls, and belongings were covered with a high proportion of respirable
519 ash with up to 8.8 wt. % cristobalite, which was isolated from the seasonal rains. We recommend that
520 hazard managers and NGOs involved in re-habitation efforts provide respiratory protection in the form
521 of disposable light weight, high efficiency masks and disseminate information on how to reduce
522 exposure, e.g., by first wetting deposits. The kitchens of most houses are commonly situated outside
523 the main living area, so indoor air pollution from cooking fires is much reduced.
524
525 **4.3 Respiratory hazard to occupational groups**
526 The number of workers and the size of the sand-mining operations indicated the importance of this
527 occupation as the main source of regular and high exposure to volcanic ash. A variable proportion of
528 adults in villages work full or part time in sand mining, with up to 20 % in a few villages. Whereas
529 deposits at other volcanoes are often quarried with heavy machinery and explosives, e.g., on
530 Montserrat, deposits at Merapi are almost entirely excavated by hand. The heavy manual labour
531 involves excavating the ash using shovels and loading it onto trucks.
532
533 Material from lahars in the area we visited was being taken directly from the river and river banks, and
534 was wet when extracted. Exposure levels for workers on site were therefore low. The lahar sample

535 investigated contained no particles smaller than 10 μm. At the sample collection distance of
536 approximately 20 km from the crater, the finer fraction had been removed in the streamflow and only
537 the coarser material was left as sediment. By the time lahars at Merapi reach approximately 20 km
538 from the summit they have deposited so much of their sediment load that they become dilute muddy
539 streamflows (Newhall et al., 2000). Further field work is required to determine whether the fines will
540 make up a more significant fraction in areas of active quarrying once the deposits begin to dry. The
541 material is mined and transported to other districts while it is still wet, but further processing of the
542 material off-site before use in construction could considerably alter the grain size and surface of the
543 material, i.e., by generating freshly-fractured crystalline silica surfaces which has been shown to
544 increase reactivity (Fubini, 1998).
545
546 The range of samples provides insight into the hazard posed by variably-sourced ash at Merapi;
547 however, the limited suite does not allow for a comprehensive definition of the occupational hazard for
548 individuals involved in mining of volcanic deposits. Crucially, we were unable to fully investigate the
549 PDC deposits as a mining hazard, such as the 18 km flow down the Kali Gendol valley, due to the
550 temperature and cohesiveness of the recently deposited unit. These pyroclastic flow deposits are
551 mined to over 10 metres depth and eventually removed from the entire channel. Much of this is fine
552 material and in dry weather there could be high exposure to the dust from directly working in the
553 deposit. To get an indication of the hazard from mining PDC deposits, we collected 16 dome rock
554 samples from the hot deposit in Kali Gendol valley deposited on 5 November. These rocks contained
555 up to 8 wt. % cristobalite, which is comparable to that seen in dome rock at Soufrière Hills volcano
556 (Horwell et al., In review). Determining which samples originated from the dome that existed prior to
557 the 26 October eruption as opposed to the new dome which grew in the lead up to the 5 November
558 eruption was difficult in the field; however, high levels of cristobalite in new dome material would
559 indicate rapid cristobalite formation in the 5 days of dome growth, in line with previous constraints by
560 Williamson et al. (2010) and Horwell et al. (In Prep-a). These results give an early indication that
561 crystalline silica may be a factor when mining PDC deposits during the dry season.
562
563 The fertile soils surrounding Merapi are intensely farmed, with nearly half of the population of the
564 Yogyakarta province dependent on agriculture for their livelihood (Wilson et al., 2007). Two of the

565 tephra fall samples were specifically collected to gain insight into the effects of volcanic ash on the
566 respiratory hazard posed to farmers (MER_10_17 and _18). MER_10_17 was taken from a flat,
567 terraced crop field, and MER_10_18 directly from vegetation. Aside from MER_10_12, these two
568 samples contained the largest proportion of fine material of all tephra fall samples (approximately 10
569 vol. % sub-4 μm material), as well as 9.2 and 4.2 wt. % cristobalite, respectively. During the field
570 mission, most ash had already dispersed from urban areas, but ash was not as quickly washed away
571 or removed in agricultural areas. In the 6 months following the eruption, however, virtually all of the
572 agricultural fields had been ploughed and reworked (John Pallister, personal communication). Ash will
573 be removed from any un-worked agricultural land through aeolian re-mobilisation of deposits as they
574 dry out and through incorporation into the soil horizons.
575
576 **4.4 Bioreactivity and health**
577 The large volume of erupted material over the southern flank of Merapi is likely to expose sand miners
578 to high levels of dust in the dry season. The cristobalite in the fine dust may be enough to adversely
579 influence the course of pulmonary tuberculosis, which is common in Indonesia (it ranks number five in
580 the world for the incidence of pulmonary tuberculosis (World Health Organisation: Regional Office for
581 South-East Asia, 2011)). Crystalline silica is known to increase the risk of developing tuberculosis and
582 to exacerbate its clinical course in certain groups of underground miners (Hnizdo and Murray, 1998;
583 teWaterNaude et al., 2006). The abundance of crystalline silica in the ash and the potential exposure
584 of the sand miners at Merapi to airborne dust warrants further investigation in the dry season. Heavy
585 dust exposure may also contribute to the development of chronic obstructive pulmonary disease,
586 especially in smokers (smoking is common in Indonesia).
587
588 Sustained inflammation in the lung plays a key role in the fibrotic changes in silicosis or mixed lung
589 fibrosis which are caused by siliceous natural dusts. Our various assays, however, showed minimal
590 bio-reactivity, indicating that the crystalline silica may be less reactive in a mixed dust or when hosted
591 in a mineral matrix, e.g., Donaldson et al. (2001). Similar results have been observed at Mt. St.
592 Helens (Vallyathan et al., 1984), Soufrière Hills (Cullen et al., 2002), despite much higher levels of
593 cristobalite (up to 20 wt. %) (Horwell et al., In Prep-a), and Rabaul (Le Blond et al., 2010). These
594 toxicity tests are not infallible guides to disease end-points and should not be taken as ruling out

595 chronic disease processes if exposure to the ash is sufficiently high. Instead, these *in vitro* tests if
596 found positive may point to disease mechanisms requiring further research: the cellular mechanisms
597 behind chronic fibrosis due to silica are still poorly understood.
598
599 Compared to other ash leachate composition, the Merapi ash samples show relatively high water-
600 soluble Zn and Cu contents (Armienta et al., 2002; Christenson, 2000; Cronin et al., 1998; Hinkley
601 and Smith, 1982). This could reflect a material which underwent prolonged exposure to high
602 temperature volcanic gases prior to the eruption (i.e., within the dome), resulting in deposition of
603 metallic compounds, predominantly as sulphate and chloride salts (Moune et al., 2010). The
604 unusually high levels of soluble Ni, Cr and Zn from MER_10_03 are higher than have been measured
605 in water leachates from other volcanoes (Geoff Plumlee, personal communication), and possibly
606 reflect ash derived from edifice/conduit/dome where intense metal deposition from hot magmatic
607 gasses occurred. The concentrations of Mn, Ni, Pb and Cd in the Merapi ash samples fall in the
608 ranges reported for other volcanoes. From a respiratory health hazard perspective, the highly soluble
609 Zn and Cu may be important. Zinc compounds such as $ZnCl_2$ may be involved in reactions with cell
610 mitochondria (e.g., Lemire et al. (2008)), while Cu may play a role in the inflammatory response of the
611 lung tissues (e.g., Rice et al. (2001)).
612
613 For this study, attendances at clinics in evacuation centres or hospital attendance data were not
614 adequate for the surveillance of patients with complaints of eye and nose irritation or acute respiratory
615 ailments.
616
617 We recommend future research to evaluate the health risk to the thousands of people employed in
618 mining and processing of the tephra-sand as aggregate for the Indonesian construction industry.
619 Aggregate mining utilizing mainly manual labour is extremely common at Indonesia's active and
620 recently active volcanoes, and, consequently, occupational exposure to volcanic particulate is likely a
621 common issue throughout the country. An exposure assessment study over the wide range of
622 activities performed by the workers on the main types of deposits should be carried out in the dry
623 season, with tephra samples concurrently collected for analysis. At least one cohort of miners should
624 be studied over time, incorporating lung function studies and symptom recording, alongside a control

625 group of non-miners. This could serve as a case study for a national level assessment of the risks
626 involved in aggregate mining, and should be undertaken alongside a study of hospital and clinic
627 routine statistics for evaluating the prevalence of TB in the Merapi area compared to non-mining
628 areas.

5. Conclusions

The October-November 2010 eruption was one of the most explosive eruptions of Mt Merapi in the past two centuries, providing unusually extensive tephra deposits, and leaving a legacy of exposure to fine ash containing low levels of crystalline silica for the thousands of people who work in the aggregate industry. There is a need to study this group further to evaluate their risk from their long term occupational exposure to ash and its effect on the common, but serious, condition tuberculosis. Our protocol, comprising a suite of mineralogical and toxicological assays, serves to better define the potential of the dust to become a respiratory hazard. Health impact studies are essential for informing officials and the public on the potential health impacts of volcanic emissions and on where to focus resources for protecting public health.

Acknowledgements

We thank the MIA-VITA team for inviting us to join their field mission. In particular, Susanna Jenkins for field mission planning and logistics, Jean-Christophe Komorowski for field assistance, and Jochen Berger for support. We were joined in the field by Estu Mei and Adrien Picquout and are indebted to them for their important collaboration in our mission, including acting as local interpreters. Estu also translated the IVHHN pamphlets into Bahasa Indonesian. We are grateful to Agung Harijoko and Bambang Widjaja, Universitas Gadjah Mada, Indonesia for field support and helpful discussion, as well as for generously organising meetings with local experts and officials. We also thank all those who were kind enough to send ash samples during and following the eruption. Our thanks to Nick March, University of Leicester, UK for XRF analyses, Chris Rolfe, University of Cambridge, UK for grain size analyses, and to the Durham GJ Russell Microscopy Facility. DD thanks the Christopher Moyes Memorial Foundation for financial support and dedication to the project. We also gratefully acknowledge Geoff Plumlee and John Pallister for their insightful reviews of the manuscript.

653 **Table Captions**

654 **Table 1:** Summary of sample information and analytical techniques carried out on each sample.
655 Further studies include: BET, EPR, iron release, haemolysis, oxidative capacity, inflammatory
656 potential, leachate. Sample MER_10_10 was excluded from the study due to a lack of eruption and
657 collection information. State of ash samples upon collection is reported in Table 2. Samples supplied
658 by [a]Agung Harijoko, Gadjah Mada University; [b]Marie Boichu, Cambridge University, and Noer Cholik,
659 BPPTK; [c]Maharani Hardjoko, Save the Children; [d]Jean-Christophe Komorowski, Institut de Physique
660 du Globe de Paris; [e]Jochen Berger, University of Hohenheim.

661 **Table 2:** Results from grain size analyses for 'respirable' (<4 μm) and 'thoracic' (<10 μm) size
662 fractions, the IAS-XRD method of quantifying cristobalite (<3 wt. % error), and BET specific surface
663 area measurements for the set of samples examined further for reactivity. Data for MER_arc are from
664 Horwell et al. (2007) and Horwell (2007) except for cristobalite content which was quantified for this
665 study.

666 **Table 3:** XRF analyses for samples MER_10_01 – MER_10_12 plus an archived sample from activity
667 in 1998 (MER_arc). Samples MER_10_01, _03, _04, _12 and _arc were collected pristine and
668 believed to be sourced from a single eruptive event. Results are organised by dry versus
669 wet/composite as the data for wet/composite samples do not necessarily reflect magmatic
670 composition. All data were collected for this study. Results are quoted as component oxide weight
671 percent and recalculated to include loss on ignition (LOI) in final total.

672 **Table 4:** Results from leachate analyses for samples MER_10_02, _03, _04 and _12.

673 **Figure Captions**

674 **Figure 1:** Protocol for rapid assessment of health hazard after Le Blond et al. (2010).

675 **Figure 2:** Location map of Merapi volcano with locations of samples analysed in this study and town
676 and river locations for geographical reference.

677 **Figure 3:** SEM images of Merapi ash showing (a) a particle which appears to be crusted with sub-
678 micron particles, and (b) a single inhalable particle with numerous sub-micron particles adhered to the
679 surface.

680 **Figure 4:** Total alkali vs. silica plot for selected Merapi samples. 'Dry ash' are samples collected fresh
681 and believed to be of a single eruptive event (MER_10_01, _03, and _04). Wet/composite are
682 samples collected following exposure to the environment and/or are believed to be composite
683 samples from multiple eruptive events (MER_10_02, _05-09, and _11). The indoor surge sample is
684 MER_10_12. MER_arc sample was collected 200 m from a PDC on the slopes of the volcano during
685 a dome collapse eruption in 1998.

686 **Figure 5:** Hydroxyl radical generation after 30 minutes against total iron released at day 7 for a
687 subset of four Merapi samples plus the 1998 ash sample (MER_arc), Min-U-Sil quartz standard, and
688 four ash samples from other volcanoes for comparison: Cerro Negro (1995), Etna (2002), Pinatubo
689 (1991), Soufrière Hills (MBA 5/6/99). Min-U-Sil quartz and MER_arc values are those published in
690 Horwell et al. (2007).

691 **References**

692 Armienta, M.A., De la Cruz-Reyna, S., Morton, O., Cruz, O. and Ceniceros, N., 2002. Chemical
693 variations of tephra-fall deposit leachates for three eruptions from PopocatÃ©petl volcano.
694 Journal of Volcanology and Geothermal Research, 113: 61-80.
695 Ayres, J.G. et al., 2008. Evaluating the Toxicity of Airborne Particulate Matter and Nanoparticles by
696 Measuring Oxidative Stress Potential—A Workshop Report and Consensus Statement.
697 Inhalation Toxicology, 20: 75-99.
698 Baxter, P.J. et al., 1999. Cristobalite in volcanic ash of the Soufriere Hills Volcano, Montserrat, British
699 West Indies. Science, 283: 1142-1145.
700 Baxter, P.J., Ing, R., Falk, H. and Plikaytis, B., 1983. Mount St. Helens eruptions: the acute respiratory
701 effects of volcanic ash in a North American community. Arch Environ Health, 38: 138-143.
702 Camus, G., Gourgaud, A., Mossand-Berthommier, P.-C. and Vincent, P.-M., 2000. Merapi (Central
703 Java, Indonesia): An outline of the structural and magmatological evolution, with special
704 emphasis to the major pyroclastic events. J. Volcanol Geotherm Res, 100: 139-163.
705 Christenson, B.W., 2000. Geochemistry of fluids associated with the 1995–1996 eruption of Mt
706 Ruapehu, New Zealand: signatures and processes in the magmatic-hydrothermal system.
707 Journal of Volcanology and Geothermal Research, 97: 1-30.
708 Cronin, S.J., Hedley, M.J., Neall, V.E. and Smith, G., 1998. Agronomic impact of tephra fallout from
709 1995 and 1996 Ruapehu volcano eruptions, New Zealand. Environmental Geology, 34(21-
710 30).
711 Cullen, R.T. et al., 2002. Toxicity of volcanic ash from Montserrat. TM/02/01, Institute of
712 Occupational Medicine, Edinburgh.
713 Donaldson, K. et al., 2001. The quartz hazard: effects of surface and matrix on inflammogenic
714 activity. J Environ Pathol Tox, 20: 109-118.
715 Expert Panel on Air Quality Standards, 1995. Particles. Department of the Environment, Her
716 Majesty's Stationery Office, London: p 30.
717 Expert Panel on Air Quality Standards, 2001. Airborne particles: what is the appropriate
718 measurement on which to base a standard? A discussion document. Department for
719 Environment, Food and Rural Affairs, London.
720 Fubini, B., 1998. Surface chemistry and quartz hazard. The Annals of Occupational Hygiene, 42: 521-
721 530.
722 Fubini, B., Mollo, L. and Giamello, E., 1995. Free radical generation at the solid/liquid interface in
723 iron containing minerals. Free Radic Res, 23: 593-614.
724 Gertisser, R., 2011. Indonesia's 'Fire Mountain' erupts. Geology Today, 27(1): 5-6.
725 Gertisser, R. and Keller, J., 2003. Temporal variations in magma composition at Merapi Volcano
726 (Central Java, Indonesia): magmatic cycles during the past 2000 years of explosive activity. J
727 Volcanol Geotherm Res., 123: 1-23.
728 Hardjosoesastro, R.R., 1956. Preliminary note on cristobalite in clay fractions of volcanic ashes.
729 Journal of Soil Science, 7(1).
730 Hillman, S.E. et al., 2012. Sakurajima volcano: a physico-chemical study of the health consequences
731 of long-term exposure to volcanic ash. Bull Volcanol.
732 Hinkley, T.K. and Smith, K.S., 1982. Leachate chemistry of ash from the May 18, 1980 eruption of
733 Mount St. Helens. U.S. Geological Survey Professional Paper, 1397-B: 27-64.
734 Hnizdo, E. and Murray, J., 1998. Risk of pulmonary tuberculosis relative to silicosis and exposure to
735 silica dust in South African gold miners. Occup Environ Med, 55(496-502).
736 Horwell, C.J., 2007. Grain size analysis of volcanic ash for the rapid assessment of respiratory health
737 hazard. J. Environ. Monitor., 9: 1107 - 1115.
738 Horwell, C.J. and Baxter, P.J., 2006. The respiratory health hazards of volcanic ash: a review for
739 volcanic risk mitigation. Bulletin of Volcanology(69): 1-24.
740 Horwell, C.J. et al., In Prep-a. Cristobalite content of ash generated by 15 years of activity of the
741 Soufrière Hills volcano, Montserrat. J Volcanol Geotherm Res.

742 Horwell, C.J., Braña, L.P., Sparks, R.S.J., Murphy, M.D. and Hards, V.L., 2001. A geochemical
743 investigation of fragmentation and physical fractionation in pyroclastic flows from the
744 Soufrière Hills volcano, Montserrat. JVGR, 109: 247-262.
745 Horwell, C.J., Fenoglio, I. and Fubini, B., 2007. Iron-induced hydroxyl radical generation from basalitic
746 volcanic ash. Earth Plan. Sci. Lett., 261: 662-669.
747 Horwell, C.J., Fenoglio, I., Ragnarsdottir, K.V., Sparks, R.S.J. and Fubini, B., 2003a. Surface reactivity of
748 volcanic ash from the eruption of Soufriere Hills volcano, Montserrat, West Indies with
749 implications for health hazard. Environ. Res., 93: 202-215.
750 Horwell, C.J. et al., In Prep-b. Respiratory health hazard assessment of the ash from the 2010
751 eruption of the Eyjafjallajökull volcano, Iceland. In Prep.
752 Horwell, C.J., Le Blond, J.S., Michnowicz, S.A.K. and Cressey, G., 2010a. Cristobalite in a rhyolitic lava
753 dome: Evolution of an ash hazard. Bulletin of Volcanology, 72: 249-253.
754 Horwell, C.J., Sparks, R.S.J., Brewer, T.S., Llewellin, E.W. and Williamson, B.J., 2003b. The
755 characterisation of respirable volcanic ash from the Soufriere Hills Volcano, Montserrat, with
756 implications for health hazard. Bull Volcanol, 65: 346-362.
757 Horwell, C.J. et al., 2010b. A mineralogical health hazard assessment of Mt. Vesuvius volcanic ash. J.
758 Volcanol Geotherm Res, 191: 222-232.
759 Horwell, C.J., Williamson, B.J., Llewellin, E.W., Damby, D.E. and Le Blond, J.S., In review. Nature and
760 formation of cristobalite at the Soufrière Hills volcano, Montserrat: implications for the
761 petrology and stability of silicic volcanic domes. Contr. Mineral. Petrol.
762 International Agency for Research on Cancer, 1997. Silica and some silicates. IARC monographs on
763 the evaluation of carcinogenic risk of chemicals to humans, Lyon, France.
764 Kobayashi, K. et al., 1993. Pyroclastic flow injury: Mount Unzen-Fugen, June 3, 1991. Japanese
765 Journal of Burn Injury, 19: 226-235 (in Japanese).
766 Lavigne, F. et al., 2011. Lahar hazards and risks following the 2010 eruption of Merapi volcano,
767 Indonesia, EGU General Assembly 2011.
768 Le Blond, J. et al., 2010. Mineralogical analyses and in vitro screening tests for the rapid evaluation of
769 the health hazard of volcanic ash at Rabaul volcano, Papua New Guinea. Bull Volcanol, 72:
770 1077-1092.
771 Le Blond, J.S., Cressey, G., Horwell, C.J. and Williamson, B.J., 2009. A rapid method for quantifying
772 single mineral phases in heterogeneous natural dust using X-ray diffraction. Powder
773 Diffraction, 24: 17-23.
774 Lemire, J., Mailloux, R. and Appanna, V.D., 2008. Zinc toxicity alters mitochondrial metabolism and
775 leads to decreased ATP production. Journal of Applied Toxicology, 28: 175-182.
776 Moune, S., Gauthier, P.-J. and Delmelle, P., 2010. Trace elements in the particulate phase of the
777 plume of Masaya Volcano, Nicaragua. Journal of Volcanology and Geothermal Research,
778 193: 232-244.
779 National Institute of Occupational Health and Safety (NIOSH), 2002. Hazard Review. Health effects
780 of exposure to respirable crystalline silica. Department of Health and Human Services.
781 National Institute of Occupational Health and Safety, Cincinnati, OH.
782 Newhall, C.G. et al., 2000. 10,000 Years of explosive eruptions of Merapi Volcano, Central Java:
783 archaeological and modern implications. J. Volcanol Geotherm Res, 100: 9-50.
784 Quality of Urban Air Review Group, 1996. Airborne particulate matter in the United Kingdom.
785 Department of the Environment, London, UK.
786 Reich, M. et al., 2009. Formation of cristobalite nanofibers during explosive volcanic eruptions.
787 Geology, 37: 435-438.
788 Rice, T.M. et al., 2001. Differential ability of transition metals to induce pulmonary inflammation.
789 Toxicology and Applied Pharmacology, 177: 46-53.
790 Surono et al., this volume. The 2010 explosive eruption of Java's Merapi volcano - a '100-year' event.
791 Journal of Volcanology and Geothermal Research.

teWaterNaude, J.M. et al., 2006. Tuberculosis and silica exposure in South African gold miners. Occup Environ Med, 63: 187-192.
Thouret, J.-C., Lavigne, F., Kelfoun, K. and Bronto, S., 2000. Toward a revised hazard assessment at Merapi volcano, Central Java. J. Volcanol. Geotherm. Res., 100: 479-502.
Vallyathan, V., Robinson, V., Reasor, M., Stettler, L. and Bernstein, R., 1984. Comparative in vitro cytotoxicity of volcanic ashes from Mount St. Helens, El Chichon, and Galunggung. J Toxicol Environ Health, 14: 641-654.
van den Bogaard, E.H.J., Dailey, L.A., Thorley, A.J., Tetley, T.D. and Forbes, B., 2009. Inflammatory Response and Barrier Properties of a New Alveolar Type 1-Like
Cell Line (TT1). Pharmaceutical Research, 26(5): 1172-1180.
Williamson, B.J., Di Muro, A., Horwell, C.J., Spieler, O. and Llewellin, E.W., 2010. Injection of vesicular magma into an andesitic dome at the effusive-explosive transition. Earth Plan. Sci. Lett., 295(1-2): 83-90.
Wilson, T., Kaye, G., Steward, C. and Cole, J., 2007. Impacts of the 2006 eruption of Merapi volcano, Indonesia, on agriculture and infrastructure.
World Health Organisation: Regional Office for South-East Asia, 2011. Tuberculosis in the South-East Asia Region.

Table 1

Table 1

Sample	Eruption Date	Collection Date	Deposit Type	Collection Location	Distance from Vent (km)	Collection Coordinates	GSA	XRF	XRD	SEM	Further Studies
MER_10_01[a]	30-Oct-10	30-Oct-10	tephra fall	Jogonalan Lor, Bantul (Rumah)	32.0 SSW	07° 49.6850 S 110° 21.0817 E	√	√	√	√	
MER_10_02[a]	26-Oct-10	31-Oct-10	tephra fall	Kepuh Harjo	5.5 S	07° 35.4928 S 110° 27.0510 E	√	√	√	√	√
MER_10_03[a]	05-Nov-10	05-Nov-10	tephra fall	Jogonalan Lor, Bantul	32.0 SSW	07° 49.6850 S 110° 21.0817 E	√	√	√	√	√
MER_10_04[b]	31-Oct-10	31-Oct-10	tephra fall	BPPTK, Yogyakarta	28.0 SSW	07° 47.8743 S 110° 23.0713 E	√	√	√	√	√
MER_10_05[c]	05-Nov-10	13-Nov-10	tephra fall	Desa Ngasem, Gulon, Magelang	18.0 SW	07° 36.1527 S 110° 17.2003 E	√	√	√		
MER_10_06[c]	05-Nov-10	13-Nov-10	tephra fall	Desa Manquncari, Sawangan, Magelang	16.0 W	07° 32.2773 S 110° 18.5593 E	√	√	√		
MER_10_07[c]	05-Nov-10	13-Nov-10	tephra fall	Desa Krogowanan, Sawangan, Magelang	11.0 W	07° 31.7755 S 110° 24.6047 E	√	√	√		
MER_10_08[c]	05-Nov-10	13-Nov-10	tephra fall	Desa Mbelan, Sawangan, Magelang	15.0 W	07° 32.6385 S 110° 18.6133 E	√	√	√		
MER_10_09[c]	05-Nov-10	13-Nov-10	tephra fall	Desa Ngadipuro, Dukun, Magelang	18.0 W	07° 33.7400 S 110° 17.2003 E	√	√	√		
MER_10_11[d]	Unknown	09-Nov-10	tephra fall	Jembatan Kali Juweh	6.0 NW	07° 29.9445 S 110° 24.6047 E	√	√	√		
MER_10_12	05-Nov-10	30-Nov-10	surge	Bronggang, Argo Mulyo	17.0 S	07° 39.7307 S 110° 27.7743 E	√	√	√	√	√
MER_10_13	05-Nov-10	30-Nov-10	surge	Bronggang, Argo Mulyo	17.0 S	07° 39.7307 S 110° 27.7743 E	√		√	√	
MER_10_14	05-Nov-10	30-Nov-10	surge	Bronggang, Argo Mulyo	17.0 S	07° 39.7407 S 110° 27.8217 E	√		√		
MER_10_15	05-Nov-10	06-Dec-10	surge	Bronggang, Argo Mulyo	17.0 S	07° 39.7407 S 110° 27.8217 E	√		√		
MER_10_16	Unknown	08-Dec-10	lahar	Siderejo (Sinduharjo)	22.0 S	07° 44.9555 S 110° 26.9088 E	√		√		
MER_10_17	Unknown	03-Dec-10	tephra fall	SW slope Merbabu, near Selo	4.5 NW	07° 34.7699 S 110° 19.4860 E	√		√		
MER_10_18	Unknown	03-Dec-10	tephra fall	SW slope Merbabu, near Selo	8.0 NW	07° 31.0715 S 110° 22.7871 E	√		√		
MER_10_19[e]	05-Nov-10	08-Dec-10	surge	N of Gadingan, E of Bronggang	17.0 S	07° 39.7367 S 110° 27.9133 E	√		√		
MER_10_20[f]	Unknown	04-Dec-10	tephra fall	S of Dukun, Magelang	12.0 W	07° 33.8713 S 110° 20.3336 E	√		√		
MER_arc	11-19 Jul 1998	09-Aug-98	tephra fall	Volcano flanks	0.2	Unknown	√	√	√		√

Table 2

Sample Name	Ash Type	Grain Size (cumulative vol. %)		Surface Area ($m^2\ g^{-1}$)	Cristobalite (wt. %)
		< 4 µm	< 10 µm		
MER_10_01	dry ash	2.7	7.6		1.9
MER_10_02	wet, composite	15.6	28.9	0.99	3.2
MER_10_03	dry ash	8.4	17.0	0.51	2.7
MER_10_04	dry ash	5.8	14.5	0.78	6.0
MER_10_05	wet, composite	6.7	14.9		3.4
MER_10_06	wet, composite	2.9	6.3		4.3
MER_10_07	wet, composite	1.4	3.0		5.5
MER_10_08	wet, composite	7.4	16.7		4.4
MER_10_09	wet, composite	7.3	15.5		4.6
MER_10_11	unknown	9.2	19.5		6.0
MER_10_12	indoor surge	13.0	25.5	1.03	8.8
MER_10_13	surge fines	19.0	35.7		3.2
MER_10_14	surge fines	19.1	35.3		4.5
MER_10_15	indoor surge	12.8	23.3		7.9
MER_10_16	lahar	0.0	0.0		3.2
MER_10_17	wet, composite	10.1	20.5		9.5
MER_10_18	wet, composite	9.7	20.8		4.2
MER_10_19	outdoor surge	6.5	13.1		3.4
MER_10_20	dry, composite	5.6	12.0		10.3
MER_arc	dry ash	12.7	27.2	1.83	3.8

Table 3

Table 3

	Sample	SiO_2	TiO_2	Al_2O_3	Fe_2O_3	MnO	MgO	CaO	Na_2O	K_2O	P_2O_5	SO_3	LOI	Total
dry	MER_10_01	55.52	0.71	18.02	7.73	0.18	1.81	6.69	3.92	2.67	0.282	0.437	1.07	99.04
	MER_10_03	54.69	0.74	19.29	7.76	0.19	2.25	8.12	3.73	2.16	0.295	0.050	0.28	99.55
	MER_10_04	56.48	0.65	18.17	6.64	0.17	1.75	6.61	4.02	2.84	0.287	0.420	1.16	99.20
	MER_10_12	55.91	0.57	19.88	5.89	0.16	1.81	7.70	3.91	2.38	0.284	0.054	0.54	99.09
	MER_arc	59.28	0.52	18.53	5.34	0.16	1.43	6.20	4.02	2.99	0.29	n/a	1.15	99.90
wet, composite	MER 10_02	57.42	0.51	19.13	5.25	0.15	1.51	6.52	4.11	2.84	0.279	0.12	1.38	99.24
	MER 10_05	52.98	0.79	18.59	8.41	0.21	2.89	9.11	3.64	2.10	0.300	0.03	0.10	99.15
	MER 10_06	53.58	0.83	18.64	8.61	0.21	2.91	8.87	3.51	1.97	0.287	0.00	0.20	99.62
	MER 10_07	51.90	1.02	17.41	10.72	0.26	3.77	9.47	3.31	1.80	0.311	<0.002	-0.02	99.95
	MER 10_08	54.37	0.75	19.29	7.86	0.20	2.67	8.52	3.75	2.19	0.273	0.01	0.11	99.98
	MER 10_09	54.75	0.73	19.04	7.53	0.19	2.48	8.32	3.71	2.23	0.266	0.234	0.31	99.78
	MER 10_10	53.45	0.82	18.93	8.72	0.21	2.89	8.98	3.52	2.03	0.280	<0.002	-0.17	99.67
	MER 10_11	53.77	0.79	19.15	8.35	0.20	2.56	8.75	3.60	2.08	0.284	0.096	0.04	99.67

Table 4

	MER_10_02	MER_10_03	MER_10_04	MER_10_12
pH	5.8	5.9	5.1	6.3
mg/kg ash				
Si	<10	20.8	181.2	53.6
Al	20.0	16.3	63.7	8.0
Fe	7.3	16.3	10.9	5.8
Mg	94	26	166	36
Ca	1900	1351	4590	1013
Na	397	87	822	167
K	110	41	189	49
Mn	20	4	31	6
F	6	17	40	12
Cl	132	192	934	49
SO_4	5450	2186	10574	1769
molal S/Cl	15.0	4.2	4.1	13.2
µg/kg ash				
As	0	0	0	0
Cd	15	12	49	3
Co	0	0	0	0
Cr	208	710	241	206
Cu	1738	1100	1188	1228
Ni	481	1415	511	453
Pb	18	42	15	27
Zn	3053	30401	4084	2753

Figure 1

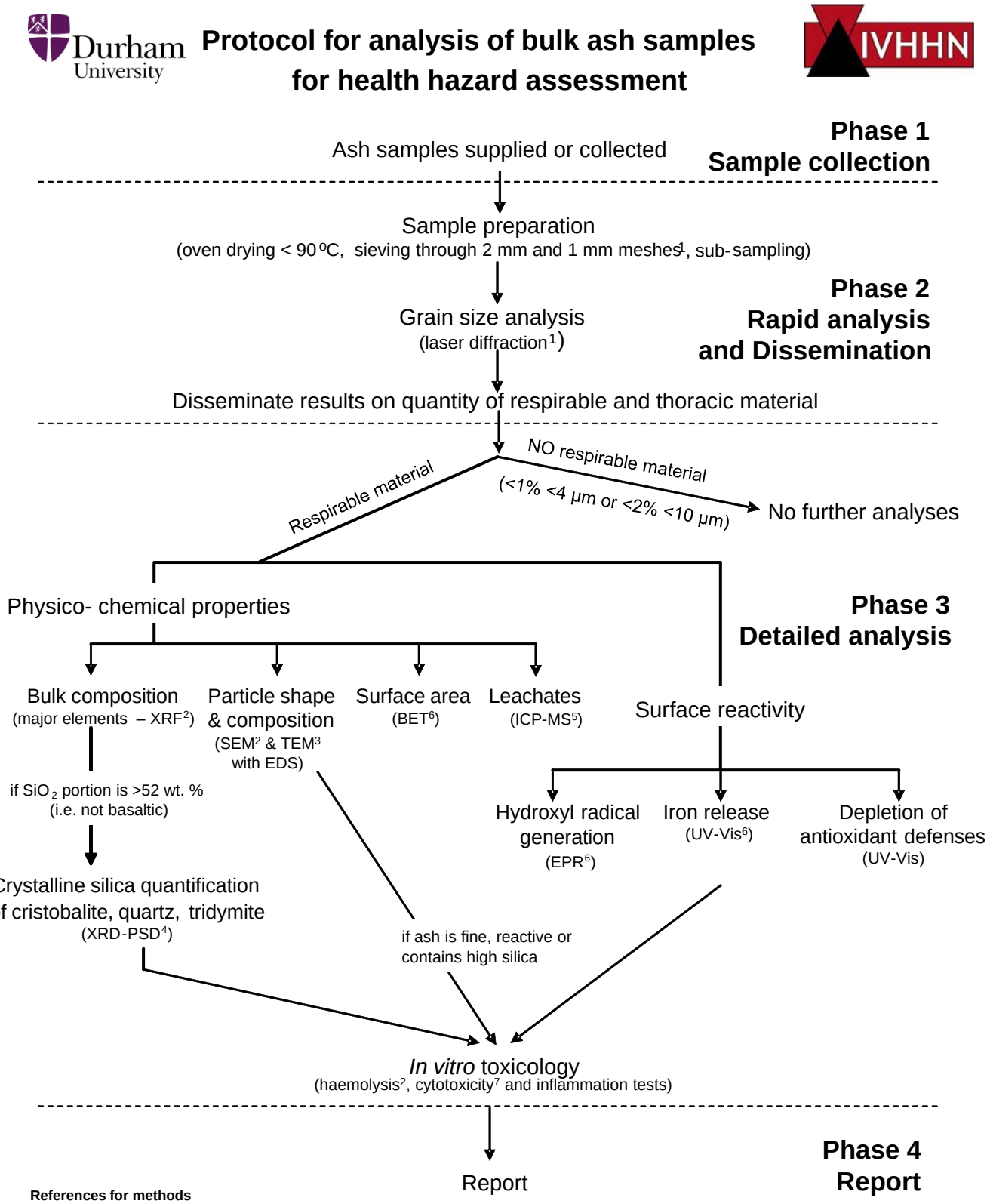

References for methods

[1] C.J. Horwell, J. Environmental Monitoring, 9 (10), 1107-1115, 2007.
[2] J.S. Le Blond, C.J. Horwell, P.J. Baxter, et al., Bulletin of Volcanology 72, 1077-1092, 2010.
[3] M. Reich, A. Zúñiga, A. Amigo, G. et al. Geology 37, 435-438, 2009.
[4] J.S. Le Blond, G. Cressey, C.J. Horwell and B.J. Williamson, Powder Diffraction 24, 17-23, 2009.
[5] C.S. Witham, C. Oppenheimer and C.J. Horwell, Journal of Volcanology and Geothermal Research 141, 299-236, 2005.
[6] C.J. Horwell, I. Fenoglio and B. Fubini, Earth and Planetary Letters 261 (3-4), 662-669, 2007.
[7] P. Ruenraroengsak, P. Novak, D. Berhanu, et al., Nanotoxicology, in press (doi: 10.3109/17435390.2011.558643), 2011.

For full references and method summaries please visit www.ivhhn.org or contact Dr Claire Horwell (claire.horwell@durham.ac.uk)

Figure 2

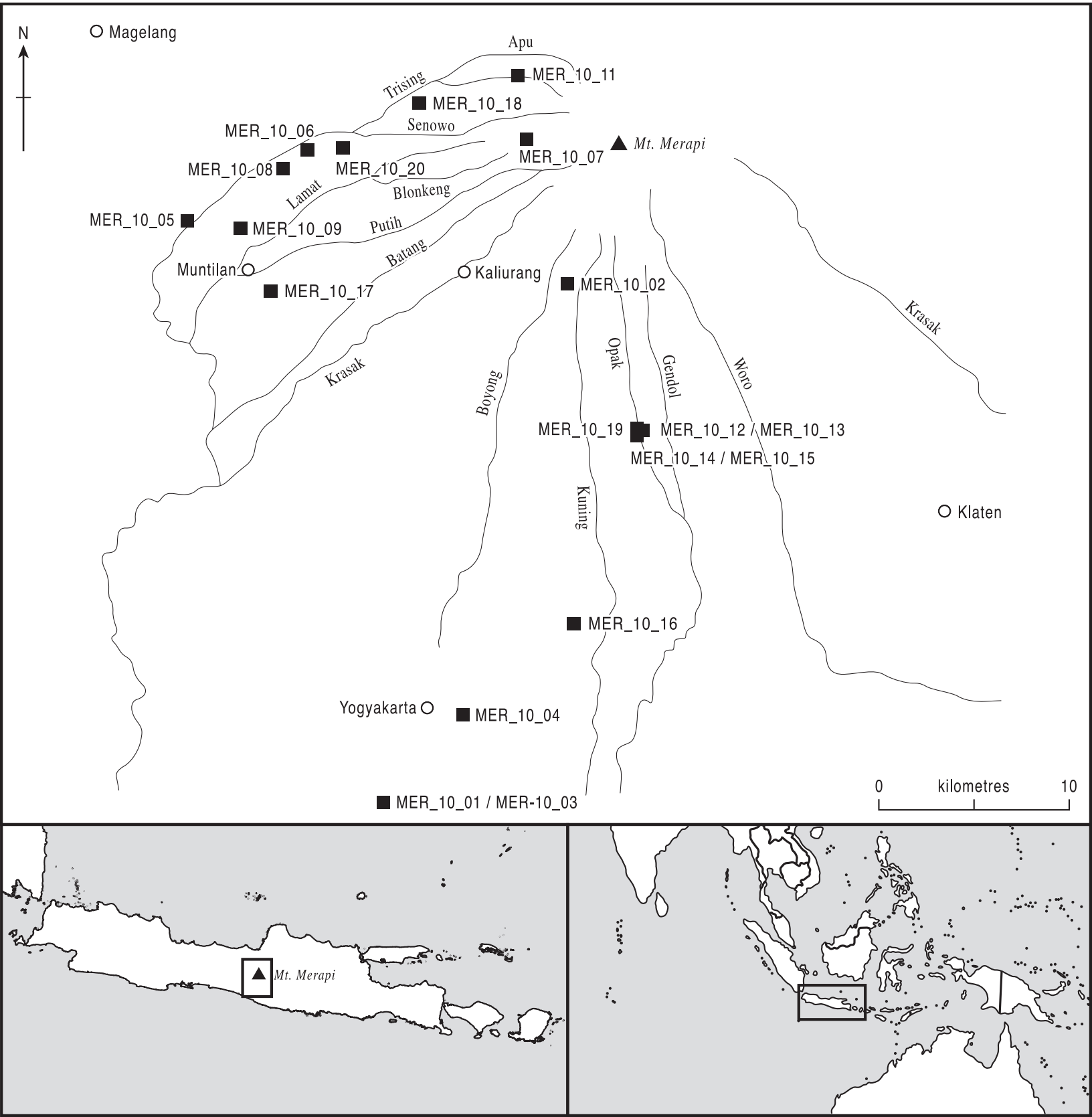
N
Magelang
Apu
Trising
MER_10_11
MER_10_18
Senowo
MER_10_06
MER_10_07
Mt. Merapi
MER_10_08
MER_10_20
Lamat
Blonkeng
MER_10_05
MER_10_09
Putih
Batang
Muntilan
Kaliurang
MER_10_02
MER_10_17
Krasak
Boyong
Opak
Gendol
Woro
Krasak
MER_10_19
MER_10_12 / MER_10_13
MER_10_14 / MER_10_15
Kuning
Klaten
MER_10_16
Yogyakarta
MER_10_04
MER_10_01 / MER-10_03
0
kilometres
10
Mt. Merapi

Figure 3

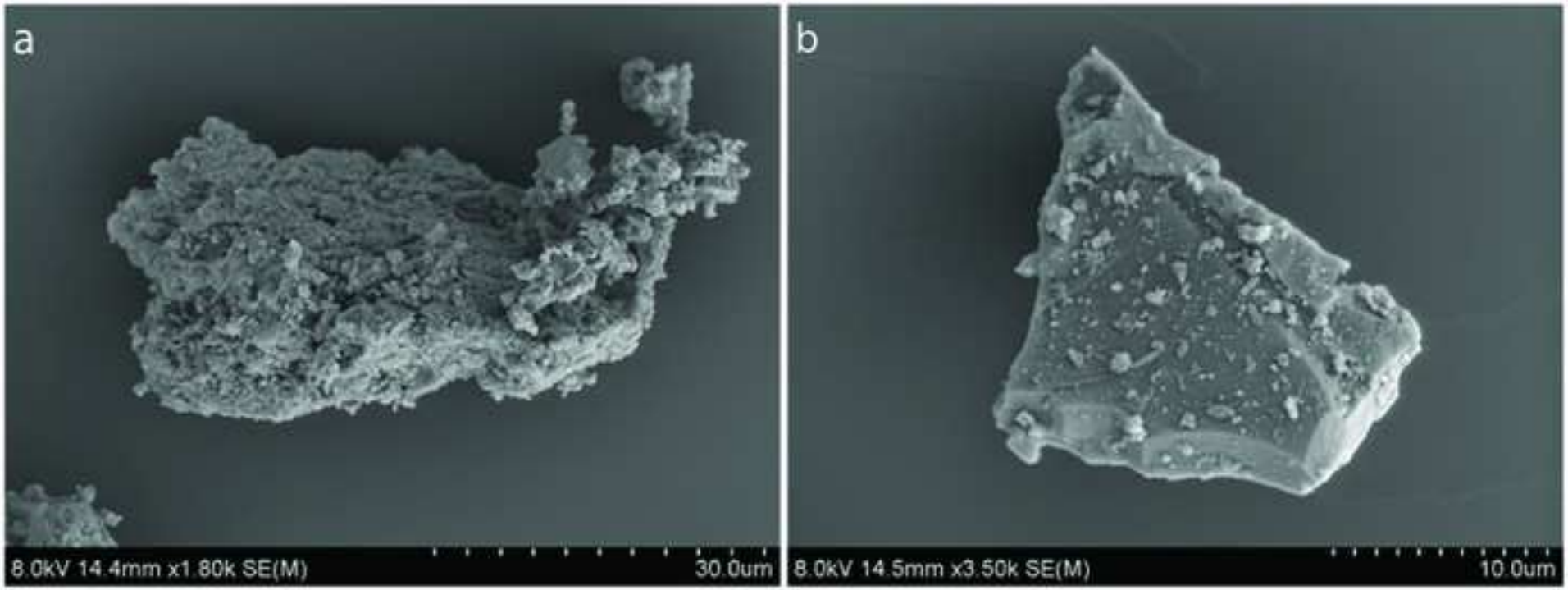

Figure 4

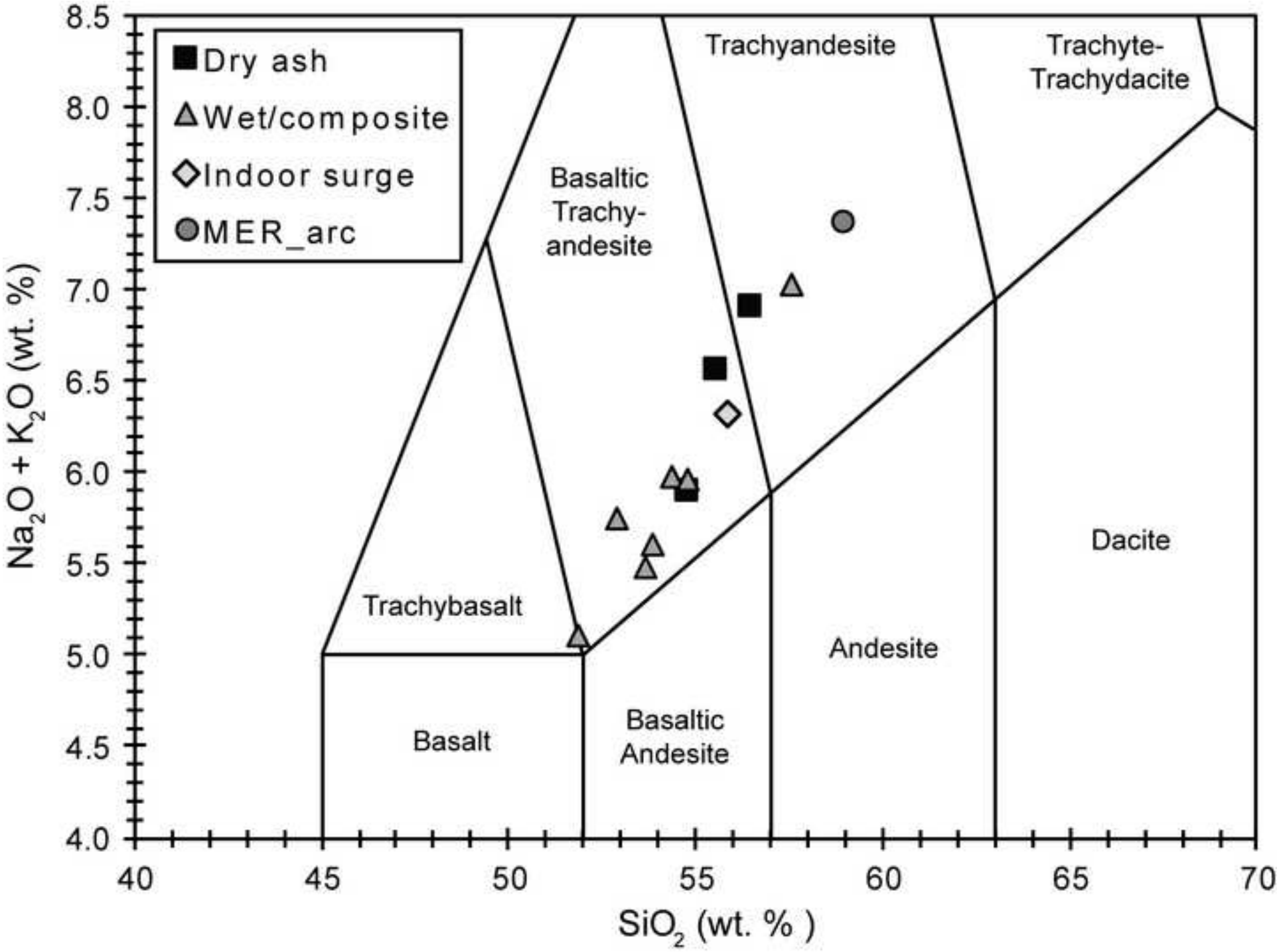
Dry ash
Wet/composite
Indoor surge
MER_arc
Trachyandesite
Trachyte-
Trachydacite
Basaltic
Trachy-
andesite
Dacite
Trachybasalt
Andesite
Basalt
Basaltic
Andesite
8.5
8.0
7.5
7.0
6.5
6.0
5.5
5.0
4.5
4.0
40
45
50
55
60
65
70
Na2O + K2O (wt. %)
SiO2 (wt. %)

Figure 5

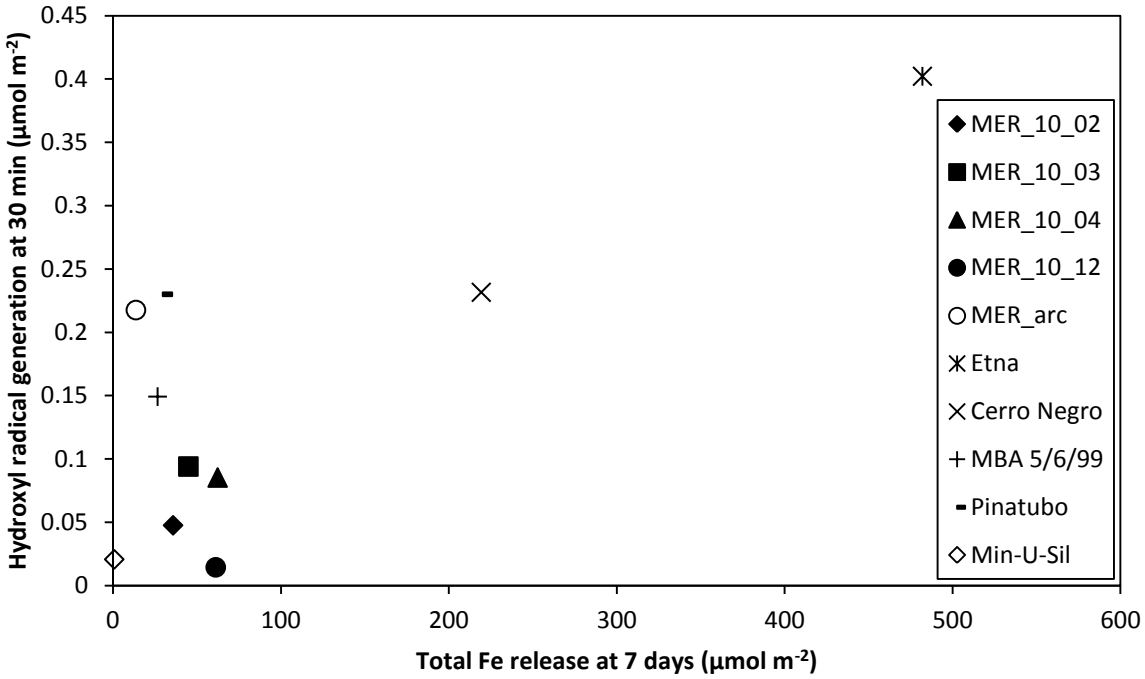
Hydroxyl radical generation at 30 min (µmol m-2)
0.45
0.4
0.35
0.3
0.25
0.2
0.15
0.1
0.05
0
0
100
200
300
400
500
600
Total Fe release at 7 days (µmol m-2)
MER_10_02
MER_10_03
MER_10_04
MER_10_12
MER_arc
Etna
Cerro Negro
MBA 5/6/99
Pinatubo
Min-U-Sil